Cell, Vol. 77, 371–379, May 6, 1994, Copyright © 1994 by Cell Press

The Drosophila *peanut* Gene Is Required for Cytokinesis and Encodes a Protein Similar to Yeast Putative Bud Neck Filament Proteins

Thomas P. Neufeld and Gerald M. Rubin
Department of Molecular and Cell Biology
Howard Hughes Medical Institute
University of California
Berkeley, California 94720-3200

Summary

We have identified a Drosophila gene, *peanut* (*pnut*), that is related in sequence to the *CDC3*, *CDC10*, *CDC11*, and *CDC12* genes of S. cerevisiae. These genes are required for cytokinesis, and their products are present at the bud neck during cell division. We find that *pnut* is also required for cytokinesis: in *pnut* mutants, imaginal tissues fail to proliferate and instead develop clusters of large, multinucleate cells. Pnut protein is localized to the cleavage furrow of dividing cells during cytokinesis and to the intercellular bridge connecting postmitotic daughter cells. In addition to its role in cytokinesis, *pnut* displays genetic interactions with *seven in absentia*, a gene required for neuronal fate determination in the compound eye, suggesting that pnut may have pleiotropic functions. Our results suggest that this class of proteins is involved in aspects of cytokinesis that have been conserved between flies and yeast.

Introduction

Organisms throughout the phylogenetic spectrum have evolved a variety of approaches to the task of cell division. Particularly diverse are the mechanisms of cytoplasmic division or cytokinesis. For example, cytokinesis in animal cells is achieved by a contractive mechanism in which a cleavage furrow forms at the cell cortex during anaphase and rapidly constricts to partition the cell. The orientation and timing of cleavage furrow formation have been shown to respond to the underlying mitotic spindle (Rappaport, 1986). In contrast, cytokinesis in most higher plants and fungi occurs by a process of vesicle fusion, in which new cell wall and membrane material is deposited between dividing cells. The division plane in these cases is established prior to nuclear division, for example, by the preprophase band of microtubules in plants (Pickett-Heaps and Northcote, 1966) and by selection of a bud site in budding yeast (Chant and Herskowitz, 1991).

The force driving the furrowing process in animal cells has been attributed to the contractile ring, a narrow band of actin filaments and bipolar myosin II filaments located adjacent to the cell membrane beneath the cleavage furrow (reviewed by Schroeder, 1990). Although clearly influenced by the spindle, the molecular nature of the signals governing assembly and function of the furrow apparatus remains a mystery. Similarly, the molecular composition of this structure has not been well established. In addition to actin and myosin, proteins such as spectrin, α-actinin, profilin, and several unidentified proteins have been shown by biochemical or immunohistochemical methods to associate with the contractile ring (Yonemura et al., 1991; Edamatsu et al., 1992), but the roles of these molecules in cytokinesis are unknown.

The budding yeast Saccharomyces cerevisiae possesses a novel cytoskeletal structure in the region of the cell where cytokinesis occurs. A ring of highly organized 10 nm filaments forms at the future site of bud emergence and is present during bud growth as a monolayer of filaments spaced at 28 nm intervals that encircle the neck region between the bud and mother cell (Byers and Goetsch, 1976a). Mutations in four cell division cycle genes, *CDC3*, *CDC10*, *CDC11*, and *CDC12*, cause a disruption of cytokinesis, giving rise to multinucleate cells with abnormal bud growth (Hartwell, 1971). The ring of 10 nm filaments is absent in these mutants (Byers and Goetsch, 1976b), suggesting that this structure plays an important role in cytokinesis. Antibodies generated against the *CDC3*, *CDC10*, *CDC11*, and *CDC12* gene products localize to the bud neck, leading to the conclusion that these genes probably encode the bud neck filament proteins (Haarer and Pringle, 1987; Ford and Pringle, 1991; Kim et al., 1991). Recently, the nucleotide sequences of *CDC3*, *CDC10*, *CDC11*, and *CDC12* have been reported (GenBank accession numbers L16548–L16551). The products of these genes define a novel family of structurally related proteins with no significant sequence similarity to other known filamentous proteins.

It is unclear whether the 10 nm filament ring reflects the specialized budding mechanism of S. cerevisiae or whether such filaments may be involved in cytokinesis in other organisms. No similar structure of highly ordered filaments has been identified in the cleavage furrows of animal cells. In this report, we describe the identification of a novel Drosophila gene, which we have named *peanut* (*pnut*), that is related in sequence to the yeast *CDC3*, *CDC10*, *CDC11*, and *CDC12* genes. We find that mutations in *pnut* cause a disruption of cytokinesis and that pnut protein is localized to the cleavage furrow of dividing cells. Our results demonstrate that this class of proteins functions in two mechanistically distinct types of cell division.

Results

pnut Is an Enhancer of *seven in absentia*

We identified the *pnut* locus in a genetic screen for mutations that disrupt photoreceptor development in the compound eye. In response to an inductive signal from an adjacent cell in the developing eye, the presumptive R7 photoreceptor normally adopts a neuronal fate (reviewed by Zipursky and Rubin, 1994). The *seven in absentia* (*sina*) gene is required for this induction: presumptive R7 cells that lack *sina* function are unresponsive to the inductive signal and fail to develop as photoreceptor neurons (Carthew and Rubin, 1990). Weak alleles of *sina* that reflect a partial loss of *sina* activity give rise to a somewhat reduced

Table 1. Enhancement of *sina* Phenotype by *pnut* Mutant Alleles

Genotype	Ommatidia Lacking R7 (%)
$pnut^{+}$/ +; $sina^{4}/sina^{4}$	22 ± 6 (n = 488)
$pnut^{1}$/ +; $sina^{4}/sina^{4}$	79 ± 10 (n = 463)
$pnut^{rN498}$/ +; $sina^{4}/sina^{4}$	37 ± 10 (n = 968)
$pnut^{rQ348}$/ +; $sina^{4}/sina^{4}$	62 ± 6 (n = 1106)
$pnut^{XP}$/ +; $sina^{4}/sina^{4}$	82 ± 7 (n = 714)

Compound eyes from adult flies of the indicated genotype were fixed and sectioned as described (Carthew and Rubin, 1990), and individual ommatidia were scored for the presence of R7 cells. n, number of ommatidia scored.

number of R7 photoreceptor cells in the adult eye. To identify factors that may interact with *sina*, we screened for dominant mutations that increase the severity of a weak *sina* allele. This screen identified nine independent mutations (R. W. Carthew, T. P. N., and G. M. R., unpublished data), including a single allele of *pnut*, $pnut^{1}$. A disruption in one of the two copies of *pnut*, by either the $pnut^{1}$ mutation or by chromosomal deficiencies for the *pnut* region, strengthens the phenotype of the hypomorphic $sina^{4}$ allele, further reducing the number of R7 photoreceptors ~4-fold (Table 1). Therefore, *pnut* formally behaves as a dominant enhancer of *sina*.

Recombination and deficiency mapping placed the *pnut* locus in the 44C region of the second chromosome. To isolate additional *pnut* alleles, a series of second chromosome P element enhancer trap lines (O'Kane and Gehring, 1987; L. S. Higgins and G. M. R., unpublished data) was tested for the ability to complement the $pnut^{1}$ mutation. We identified two lines, *rN498* and *rQ348*, that fail to complement $pnut^{1}$; each contains a single P element insertion at cytological position 44C1-2 (data not shown). Each line also behaves as a dominant enhancer of *sina*, albeit to a lesser degree than the $pnut^{1}$ mutation (Table 1). A molecular null allele was generated by imprecise excision of the *rN498* P element. This allele, $pnut^{XP}$, which lacks nearly all of the *pnut* coding region (see legend to Figure 3), was used for the phenotypic analysis described below.

pnut Is Required for Cytokinesis

Homozygous $pnut^{XP}/pnut^{XP}$ ($pnut^{-}$) animals do not survive to adulthood but instead die shortly after pupation. Dissection of $pnut^{-}$ third instar larvae revealed severely reduced imaginal discs, the epithelial structures that give rise to adult tissues. In most cases no discs could be seen under the dissecting microscope. Gatti and Baker (1989) have shown that such a discless, pupal-lethal phenotype often reflects an underlying defect in mitosis. In such mitotic mutants, early divisions during embryogensis are presumably supported by maternally supplied gene products, but later proliferation of imaginal tissues is dependent on the mutant zygotic genome. To look for mitosis defects in *pnut* mutants, we examined nuclei from orcein-stained brain preparations of third instar $pnut^{-}$ larvae. The number of neuroblasts undergoing mitosis in $pnut^{-}$ brains is similar to that of wild-type controls, indicating that initiation of mitosis is not impaired. Chromosome condensation and anaphase separation also appear normal. However, $pnut^{-}$ brains contain a large number of polyploid cells. Most of these cells are tetraploid (Figure 1B), but occasionally we observed nuclei with ploidy of eight or greater (Figure 1C). The absolute number of polyploid cells is variable, but such cells were observed in all $pnut^{-}$ brains examined. In addition, cells containing two metaphase nuclei were often observed (data not shown).

This pattern of mitotic defects is similar to those of previously described Drosophila mutations that disrupt cytokinesis (Gatti and Baker, 1989; Karess et al., 1991). To determine whether the proliferation defect observed in $pnut^{-}$ imaginal discs is due to a disruption of cytokinesis, we examined the nucleus to cell ratio of these tissues. Imaginal discs from wild-type and $pnut^{-}$ third instar larvae were double labeled with a rabbit polyclonal serum against Drosophila α-spectrin, which labels the cell membrane, and

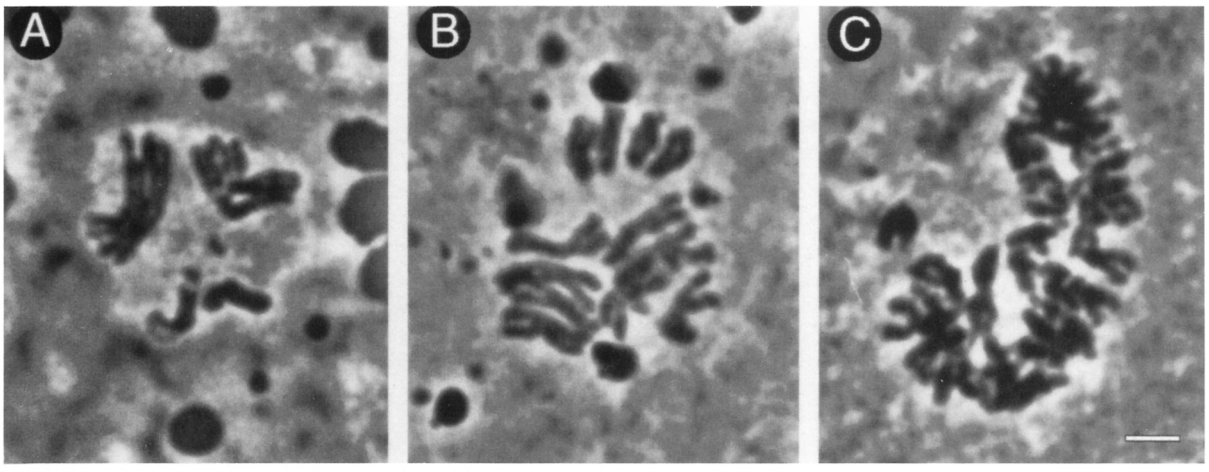

Figure 1. Metaphase Chromosomes from Wild-Type and $pnut^{-}$ Third Instar Larval Neuroblasts

(A) Wild-type diploid cell with a pair of telocentric X chromosomes and two pairs of metacentric autosomes. (B) $pnut^{-}$ tetraploid cell. (C) Approximately octaploid $pnut^{-}$ cell. Scale bar, 2 μm.

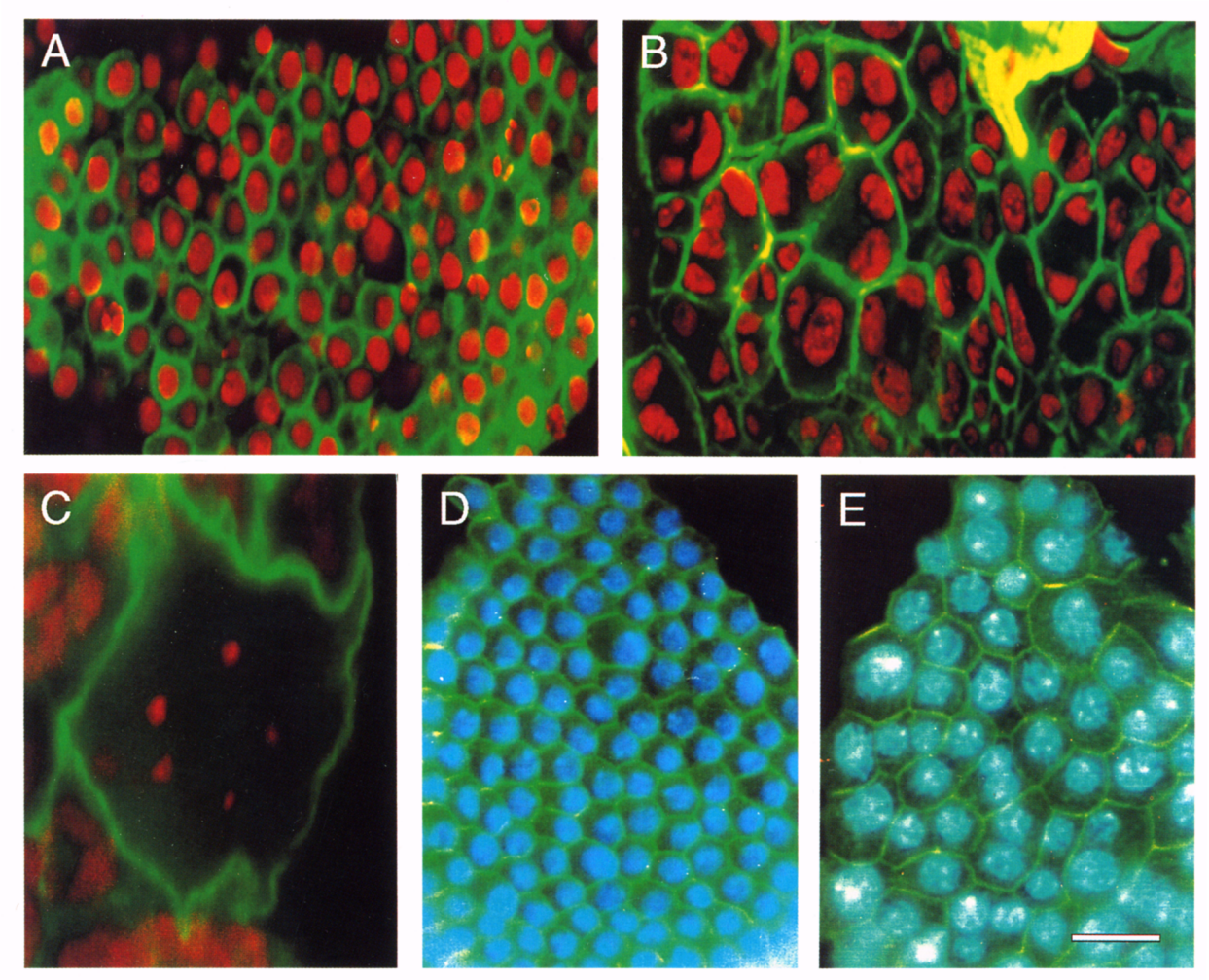

Figure 2. Multinucleate Cells in *pnut*⁻ Tissues

(A) Confocal image of a wild-type lymph gland stained with anti-α-spectrin antibody (green), which labels the cell membrane, and with the nuclear dye propidium iodide (red).

(B) *pnut*⁻ lymph glands stained as above. The majority of *pnut*⁻ cells are of larger size than wild type and often contain multiple nuclei.

(C) *pnut*⁻ leg imaginal disc cell stained with anti-α-spectrin antibody (green) and with the centrosome-specific antibody anti-DMAP60 (red). This image is a superimposition of six confocal optical sections. The DMAP60 antibody identifies five centrosomes in this cell.

(D and E) Fluorescent photomicrographs of wild-type (D) and *pnut*⁻ (E) ovarian follicle cells stained with anti-α-spectrin antibody (green) and the nuclear dye Hoechst 33258 (blue).

Scale bar in (E) represents 15 μm in (A) and (B), 5 μm in (C), and 25 μm in (D) and (E).

with the nuclear dye propidium iodide. These preparations were then examined by confocal microscopy. This method provides clear identification of cell outlines and allows determination of the number of nuclei per cell. Wild-type tissues prepared in this way contain cells of uniform size with single nuclei (Figure 2A). In contrast, *pnut*⁻ tissues contain a large number of multinucleate cells, with two to six nuclei per cell (Figure 2B). These cells range in size from an approximately normal 5 μm to greater than 20 μm in diameter. Nuclei in the larger cells are also considerably larger than normal diploid nuclei and are presumably polyploid. In addition, staining of *pnut*⁻ imaginal tissues with an anti-β-tubulin antibody (data not shown) or with an antibody that localizes to centrosomes (anti-MAP60; Figure 2C) revealed cells with multipolar mitotic spindles and extra centrosomes. We found large, multinucleate cells in all *pnut*⁻ imaginal tissues examined, with the most severe effects seen in the lymph glands and imaginal rings of the salivary glands, in which nearly all cells contain multiple nuclei. Similar defects were also observed in the ovarian follicle cells of *pnut* mutants. *pnut*⁻ flies carrying a P element construct that places expression of the *pnut* gene under the control of the Drosophila *hsp70* promoter (see Experimental Procedures) can be rescued to adulthood by providing *pnut* expression during development by heat shock. Transformants placed at a noninducing temperature (22°C) as adults are sterile, and the ovaries of such females progressively degenerate (data not shown). Membrane and nuclear staining of these ovaries revealed several follicle cells with multiple large nuclei (Figure 2E).

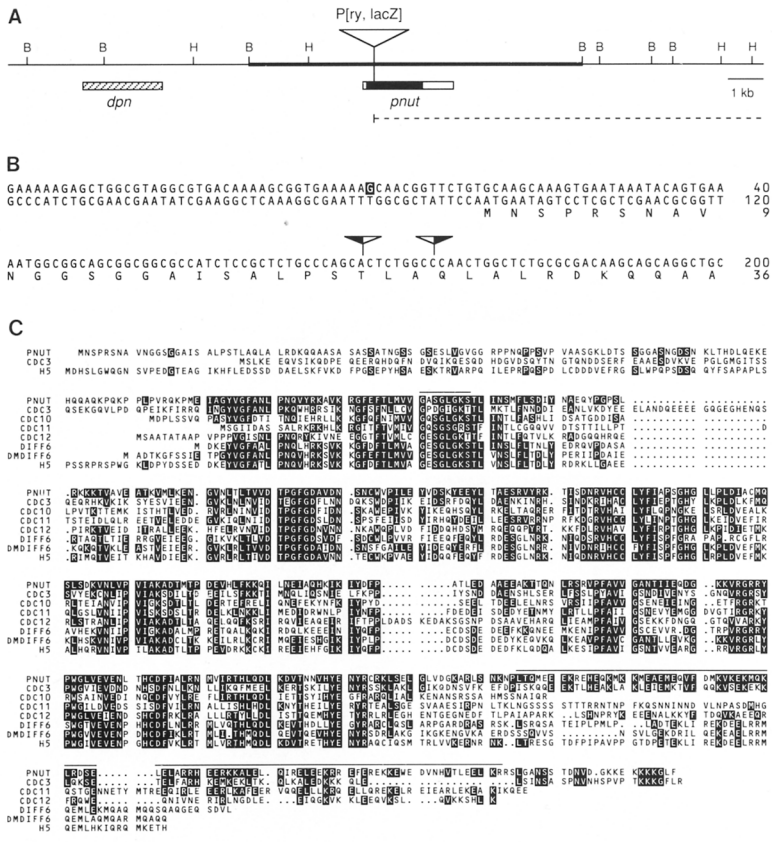

Figure 3. Genomic Organization at the *pnut* Locus

(A) Restriction map of cloned phage genomic DNA. The *pnut* transcript is represented by a bar, with the closed region of the bar representing the coding sequence. The insertion site of the *rN498* and *rQ348* P elements in the 5′ end of the *pnut* transcript is shown. The *deadpan* (*dpn*) transcription unit is represented by the hatched bar. The 10 kb BamHI fragment used for transformation rescue of *pnut*^{XP} is depicted as a bold line. The region of DNA deleted in the *pnut*^{XP} excision allele is represented by the broken line. This deletion begins at the insertion site and extends downstream beyond the region of genomic DNA shown here. The distal limit of the deletion was not determined. It extends at least 17 kb, but cannot contain any other essential genes as its lethality can be rescued by both *pnut* rescue constructs. Restriction enzyme abbreviations: B, BamHI; H, HindIII.

(B) Nucleotide sequence of the *pnut* transcript 5′ end and upstream genomic DNA. The first nucleotide of the 2.5 kb cDNA is boxed and is designated as +1. The insertion sites of the *rN498* and *rQ348* P elements are represented by triangles. P element orientation is indicated by the closed half of the triangle, which represents the region of the PZ element (Mlodzik and Hiromi, 1991) that is included in the rescue plasmid.

(C) Predicted amino acid sequence of the pnut protein. Conceptual translation of the long open reading frame of the *pnut* 2.5 kb cDNA produces a 539 amino acid polypeptide of 60 kDa. The predicted pnut sequence is compared with the sequences of seven related proteins: the Cdc3p, Cdc10p, Cdc11p, and Cdc12p proteins of S. cerevisiae (GenBank accession numbers L16548–L16551); two murine proteins, Diff6 and H5 (Nottenburg et al., 1990; Kato, 1991); and a Drosophila Diff6 homolog, DmDiff6 (GenBank accession number X67202). Residues identical to the pnut sequence are boxed. The P loop motif (amino acids 149–156) and putative coiled-coil region (amino acids 427–515) are overlined.

Taken together, these results strongly indicate that the failure of proliferation observed in *pnut*$^{-}$ imaginal tissues is due to a defect in cytokinesis.

Isolation of the *pnut* Gene

To initiate the molecular cloning of *pnut*, genomic DNA adjacent to the *rN498* and *rQ348* P insertions was recovered by plasmid rescue in Escherichia coli (Pirrotta, 1986) and used to screen a Drosophila genomic DNA library. DNA blotting and restriction analysis of DNA from this region demonstrated that the two P elements had inserted at nearly identical sites, ~5 kb upstream of the *deadpan* gene (Figure 3A). Genomic DNA flanking the insertion sites was used to screen a cDNA library prepared from eye–antennal imaginal disc RNA. Six related cDNA clones, ranging in size from 1.2 to 2.5 kb, were isolated. The three largest cDNA clones spanned the P insertion point, indicating that the P elements had inserted into this transcription unit. The precise site of P element insertion was determined by sequencing the junctions between P element and genomic DNA. We found that the two P elements are located 8 nt apart, in the coding region near the 5′ end of the transcript (Figure 3B). The largest cDNA was used to probe a blot of imaginal disc RNA and hybridized to a single transcript of 2.5 kb (data not shown), indicating that we had cloned an approximately full-length transcript. Comparison of the nucleotide sequences of the cDNA and corresponding genomic region revealed an absence of introns in this transcript.

To confirm that the 2.5 kb cDNA corresponds to the *pnut* transcript, we introduced DNA from this region into *pnut*$^{-}$ flies by P element–mediated germline transformation. Two rescue constructs were used. The first contained a 10 kb genomic fragment encompassing the 2.5 kb transcription unit (Figure 3A). This construct completely rescues *pnut*$^{-}$ mutants to full viability and fertility. The second construct contained the coding region of the 2.5 kb transcript subcloned into the pHS-CaSpeR vector, which carries the Drosophila *hsp70* promoter (Pirrotta, 1988). Rescue of *pnut*$^{-}$ flies carrying this construct requires induction by heat shock (every 24 hr for 1 hr at 38°C) during larval and pupal development. As further confirmation that we had correctly identified the *pnut* transcription unit, protein immunoblot analysis using monoclonal antibodies (MAbs) generated against a product of the 2.5 kb cDNA identified a single protein species of 60 kDa that is present in wild-type larval extracts and absent in *pnut*$^{-}$ extracts (data not shown). These data demonstrate that the 2.5 kb transcription unit corresponds to *pnut*.

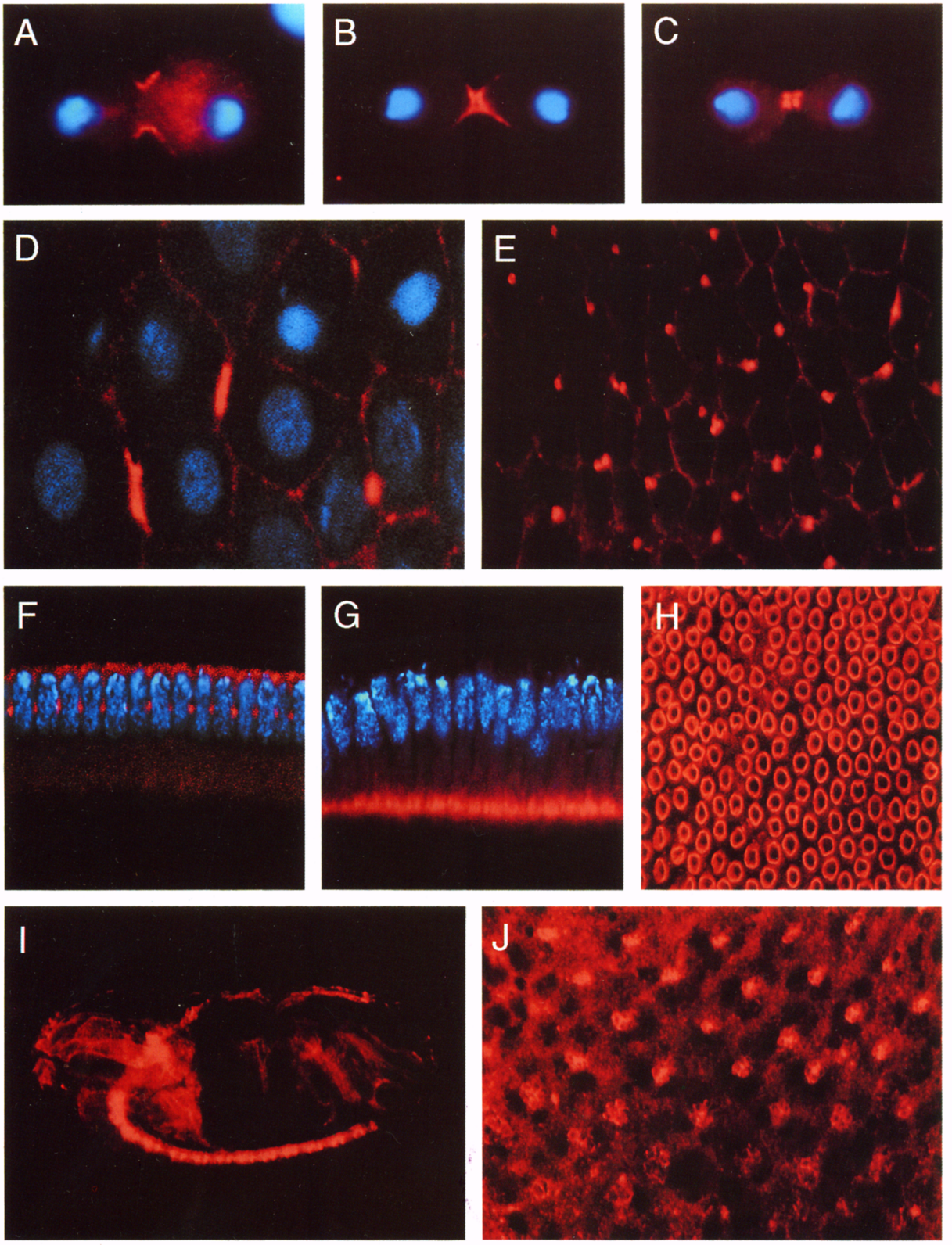

Figure 4. Pnut Protein Localization

Cells were fixed as described and stained with MAb 4C9, an antibody raised against the amino-terminal 116 amino acids of the pnut protein.

(A–C) Fluorescent photomicrographs of Drosophila S2 cells in progressive stages of cytokinesis stained with MAb 4C9 and Hoechst 33258. (A) S2 cell during early furrow formation, with a slight concentration of MAb 4C9 staining at the furrow membrane. (B) Cell nearing completion of furrowing with intense staining of the cleavage furrow. (C) Postmitotic daughter cells with staining of the intercellular bridge. Note the absence of staining in the midbody.

(D–I) Confocal images of MAb 4C9–stained Drosophila embryos. Nuclei were labeled with chromomycin A. Embryos in mitotic cycle 14 display a low level of general membrane staining and a concentration of staining in cleavage furrows (D) and intercellular bridges (E). During cellularization of the syncitial blastoderm, pnut protein is localized to the advancing membrane front (F) and becomes highly concentrated in the cytoplasmic connections between cells and yolk following cellularization, as seen in longitudinal (G) and tangential (H) views. (I) shows a 14 hr embryo with staining localized to the ventral nerve cord.

(J) Confocal image of a third instar eye imaginal disc stained with MAb 4C9, showing concentrated staining in the apical membranes of developing photoreceptor cells.

pnut Is Similar to the Bud Neck Filament Genes of S. cerevisiae

Nucleotide sequencing of the 2.5 kb *pnut* cDNA revealed a single open reading frame of 1617 bp predicted to encode a 539 amino acid polypeptide of 60 kDa (Figure 3C). Searches of the current data bases revealed a similarity to the *CDC3*, *CDC10*, *CDC11*, and *CDC12* gene products of the budding yeast S. cerevisiae (GenBank accession numbers L16548–L16551). These genes are required for cytokinesis and are thought to encode components of a ring of 10 nm filaments located at the bud neck (see Introduction). Similar proteins have recently been identified in mouse (Diff6 and H5; Nottenburg et al., 1990; Kato, 1991) and Drosophila (Dmdiff6; GenBank accession number X67202), but the role of these proteins has not been determined.

The sequence identity between pnut and these proteins ranges from 35% for Cdc11p to 54% for Dmdiff6, over a region of 300–400 amino acids (Figure 3C). Three of the proteins, pnut, Cdc3p, and H5, contain amino termini of ~100 amino acids with limited sequence similarity. None of the proteins shows significant sequence identity to known filamentous proteins. However, an algorithm that predicts the likelihood of coiled-coil structure based on comparison to the sequences of known coiled-coil domains (Lupas et al., 1991) finds a high probability of such a domain in the carboxyl terminus of most of these proteins, including pnut (residues 427–515; $p > 0.97$). In addition, each of these proteins contains an ATP/GTP-binding site motif (P loop; Saraste et al., 1990) that may be involved in their assembly or regulation.

Pnut Protein Is Localized to the Cleavage Furrow of Dividing Cells

MAbs generated against a glutathione S-transferase (GST)–pnut fusion protein were used to label Drosophila S2 tissue culture cells (Figures 4A–4C). Cells in interphase stain at a low intensity, with a slight concentration of staining at the plasma membrane. Localization of this staining first occurs in late anaphase cells, as membrane staining increases at the newly forming cleavage furrow (Figure 4A). Such staining was only observed in cells that had initiated cleavage. The intensity of staining at the furrow increases as it progresses inward (Figure 4B) and appears to occur at the expense of overall membrane staining, which decreases during cytokinesis, suggesting that pnut protein may be recruited to the furrow from other regions of the membrane. Following mitosis, staining persists well into interphase at the intercellular bridge connecting daughter cells (Figure 4C).

A staining pattern essentially identical to this was observed in dividing cells of the embryo and imaginal discs. Gastrulation stage embryos labeled with anti-pnut MAbs show a general membrane staining of interphase cells, with staining concentrated in the cleavage furrows of dividing cells (Figure 4D) and the cytoplasmic bridges connecting postmitotic daughter cells (Figure 4E). Prior to the cellular blastoderm stage, the embryo exists as a syncitium of nuclei that undergoes cellularization following mitotic cycle 13. This process resembles cytokinesis in some aspects, and the advancement of membranes between the syncitial nuclei is comparable to furrowing in dividing cells (reviewed by Schejter and Wieschaus, 1993). Following cellularization, the newly formed cells remain connected for several minutes to the underlying yolk by narrow cytoplasmic channels. Embryos of these stages stained with anti-pnut antibodies show intense staining of the advancing membrane front and of the later yolk connections (Figures 4F–4H), suggesting that pnut may have a role in cellularization similar to its function during cytokinesis. In addition, we detected a high level of diffuse staining in 0–2 hr embryos (data not shown), presumably reflecting maternally supplied pnut protein.

Intense staining was also detected on the cell surfaces of the embryonic central nervous system and on the apical membranes of developing photoreceptor cells in the eye imaginal disc (Figures 4I–4J). We also observed punctate cytoplasmic staining in a subset of eye disc and larval central nervous system cells (data not shown).

Discussion

The morphological aspects of mitosis in budding yeast are quite distinct from those of higher eukaryotes. In yeast cells, no furrowing process occurs. Rather, a new bud begins to emerge near the beginning of S phase (Hartwell, 1974) and grows continuously throughout the cell cycle. Following DNA replication, the nucleus migrates to the neck between the mother cell and bud, where it elongates and eventually divides. Cytokinesis is finally accomplished in the neck region by fusion of vesicles with the cell membrane (Byers and Goetsch, 1976a). Throughout this process, the diameter of the neck and underlying ring of 10 nm filaments remains constant (Byers and Goetsch, 1976a), and no contractile activity is evident. In contrast, the furrow apparatus of animal cells forms only after the onset of anaphase and then rapidly contracts to bisect the cell. Following the completion of furrowing, the contractile ring of actin filaments disassembles (Schroeder, 1972), leaving the daughter cells connected by a narrow intercellular channel for up to several hours (Byers and Abramson, 1968; Sanger et al., 1985).

Despite these mechanistic differences in division between flies and yeast, we have found that mutations in *pnut* cause a disruption of cytokinesis similar to that of the *cdc3*, *cdc10*, *cdc11*, and *cdc12* mutants. Moreover, pnut protein localizes to a ringed structure in the region of cytokinesis, as do the products of the neck filament genes. We do not know whether these similarities are serendipitous or whether they reflect functions conserved between the Drosophila and yeast proteins. No structure resembling the coil of regularly spaced 10 nm filaments has been reported in cleavage furrows. However, electron micrograph studies of the intercellular bridge connecting pairs of daughter cells from a human bone marrow cell line (Mullins and Biesele, 1977) identified segments of the bridge in which the membrane was organized into wavelike ripples with a distinct periodicity of 34–43 nm, although no underlying repeating structures were observed. In addition, electron micrographs of similar bridges between Dro-

sophila embryonic cells (Rickoll and Counce, 1980) revealed electron-dense material adjacent to the cell membrane with a periodicity of ~60 nm, suggestive of a similar structure of coiled filaments. We find that anti-pnut antibodies strongly stain these bridges in embryonic and imaginal disc cells (Figure 4E). Moreover, antisera raised against a second Drosophila neck filament homolog, Dmdiff6, localize in a pattern identical to that of anti-pnut antibodies (J. Fares and J. Pringle, personal communication), suggesting that pnut and Dmdiff6 may assemble into a multicomponent structure as in S. cerevisiae.

The role of the bud neck filaments in yeast cytokinesis is not known, although several possibilities have been proposed. Byers and Goetsch (1976a) have suggested that the filamentous ring either may play a structural role, counteracting the outward pressure on the cell surface in the neck region, or may be involved in the localization of specific components to this area, such as factors required for cell wall deposition. Each of these activities, modified to a more general level, could also be applicable to a role in contractive cytokinesis. Following disassembly of the contractile ring, the cell membrane remains constricted about the microtubules spanning the intercellular bridge. Filaments of 10 nm may be involved in maintaining the narrow dimensions of the cell in this region after the actin filaments have been disassembled. The bud neck of yeast cells and the intercellular bridge of animal cells are both ~0.5 μm in diameter (Byers and Goetsch, 1976a; Mullins and Biesele, 1977; Rickoll and Counce, 1980), and perhaps the 10 nm filaments are specially adapted to form a structure of this size. Alternatively, these proteins may act earlier to localize actin or other components of the contractile ring to the presumptive cleavage furrow. Our observations do not allow us to distinguish between these possibilities. Comparison of pnut protein localization with that of filamentous actin, as detected by rhodamine-conjugated phalloidin, detected no differences in the timing of arrival at the cleavage furrow (data not shown); concentration of neither protein was observed in the cleavage plane cortex prior to the onset of furrowing.

Two additional Drosophila mutants that specifically affect cytokinesis have been described. Mutations in *spaghetti-squash* and *pebble* result in a disruption of cytokinesis with no effect on earlier stages of the cell cycle (Karess et al., 1991; Hime and Saint, 1992; Lehner, 1992). The terminal phenotype of *spaghetti-squash*, which encodes the nonmuscle myosin light chain, is similar to that of *pnut*, with a pupal-lethal phase and rudimentary imaginal discs (Karess et al., 1991). The relatively late timing of such defects in *spaghetti-squash* and other mitotic mutants has been attributed to the action of maternal gene products during embryonic divisions. Our finding of pnut protein in the early embryo prior to zygotic transcription lends support to this idea. In contrast, zygotic transcription of *pebble* is required for cytokinesis during embryonic cell divisions (Lehner, 1992; Hime and Saint, 1992).

We originally identified mutations in *pnut* by their effect on photoreceptor development. A disruption in one of the two copies of *pnut* (presumably resulting in a 50% reduction in the level of the *pnut* translational product) increases the severity of a weak *sina* allele ~4-fold, suggesting that the level of *pnut* activity is a limiting factor in signaling through *sina*. In light of the role of *pnut* in cytokinesis, one interpretation of these results is that a reduction in *pnut* activity causes a delayed exit from mitosis, leaving the presumptive R7 cell in a state refractive to inductive signaling. R7 induction is immediately preceded by a final round of cell division (Wolff and Ready, 1991), and studies with temperature-sensitive alleles of *sevenless* (Mullins and Rubin, 1991) have shown that successful induction requires a continuous signal for a period of 6 hr following this final cell division. Therefore, even a slight delay in the cell cycle due to reduced *pnut* activity may be enough to decrease further the ability of the presumptive R7 cell in *sina*^{4} flies to respond properly to inductive signals.

Alternatively, the effect of *pnut* mutations on cell signaling may reflect the pleiotropic functions of this family of proteins. In addition to defects in cytokinesis, *cdc3*, *cdc10*, *cdc11*, and *cdc12* mutants display a disruption in the positioning of new bud sites (Flescher et al., 1993). One model of bud site selection proposes that factors remaining at the previous site of cytokinesis direct assembly of components required to form a new adjacent bud (Chant and Herskowitz, 1991; Snyder et al., 1991). In this view, a general role of the 10 nm filaments would be to localize specific factors to defined regions of the cell membrane: to the bud neck in the case of cytokinesis and to a position adjacent to the previous filament ring in the case of bud site selection. In this regard, murine *Diff6* was isolated in a screen for molecules whose abundance varied with that of a cell surface glycoprotein involved in lymphocyte homing (Nottenburg et al., 1990). In addition to the localization of pnut protein in the cleavage furrow, we find that it is concentrated at the apical surfaces of developing photoreceptors in the eye imaginal disc and at the cell membranes of neurons in the embryonic ventral nerve cord. Pnut may be acting in these cases to localize molecules, such as components of the signaling apparatus, to specific domains of the cell surface.

Experimental Procedures

Genetics

The mutagenesis screen for dominant enhancers of *sina* will be described elsewhere (R. W. Carthew, T. P. N., and G. M. R., unpublished data). In brief, *sina*^{4} *tld/TM1 kni* males were mutagenized with EMS and crossed to *sina*^{4} *kni/TM3 tld* females. F1 progeny (*sina*^{4} *tld/sina*^{4} kni) were anesthetized and assayed for the presence of R7 photoreceptors by the reduced corneal pseudopupil method (Franceschini and Kirschfeld, 1971). We screened ~30,000 flies. The second chromosome mapping stock (*al dp b pr c px sp*) was used to determine the meiotic position of the *pnut*^{1} mutation. The map position was further refined by inclusion in the deficiencies *Df(2R)44CE* and *Df(2R)193A* (Hooper and Scott, 1989). These deficiencies fail to complement the recessive lethality associated with the *pnut*^{1} chromosome and behave as strong dominant enhancers of *sina*.

Recessive lethal lines *rN498* and *rQ348*, containing the P[*lacZ, ry*$^+$] element (PZ element; Mlodzik and Hiromi, 1991) came from a collection of enhancer trap lines with β-galactosidase expression patterns in the eye imaginal disc (L. S. Higgins and G. M. R., unpublished data). The *rN498* P element was mobilized by introducing a chromosome carrying the Δ2-3 source of transposase activity (Robertson et al., 1988). Of 248 lines that lost the *ry*$^+$ marker associated with the P[*lacZ, ry*$^+$] element, 19% reverted to viability, indicating that the recessive

lethality of *rN498* was due solely to the P element insertion. Two ry^+ nonrevertant lines that carry small deletions in the *pnut* region were identified by PCR and DNA blot analysis. One of these lines, designated $pnut^{XP}$, lacks all *pnut* sequences downstream of the *rN498* P insertion site (located 75 bp into the *pnut* coding region).

The $pnut^{XP}$ chromosome was kept over the compound balancer SM6-TM6b that carries the dominant body-shape marker *Tubby*. This allowed us to distinguish homozygous $pnut^{XP}$ third instar larvae (phenotypically non-*Tubby*) from their heterozygous siblings (phenotypically *Tubby*).

Cytological Examination of Dividing Cells

Aceto-orcein squashes of third instar larval ganglia were prepared as follows. Brain complexes from homozygous $pnut^{XP}$ third instar larvae or heterozygous controls were dissected in 0.1 M NaCl, transferred to 50% acetic acid for 30 s, and placed in a drop of 2% natural orcein (Bio/medical Specialties) in 50% acetic acid on a siliconized slide for 5 min. The stained brain complexes were squashed under a siliconized coverslip and examined with phase-contrast optics.

Molecular Biology

All nucleic acid labeling and hybridization procedures were performed with nonradioactive techniques. Digoxigenin-labeled DNA probes were made and detected according to the the specifications of the manufacturer (Genius System, Boehringer Mannheim).

Genomic DNA fragments of 0.8 and 3.0 kb flanking the *rN498* and *rQ348* P elements were isolated by plasmid rescue as described (Pirrotta, 1986). These fragments were used to probe a Drosophila genomic DNA library in λFIX (Stratagene) made by K. Moses. Seven overlapping clones were recovered, and a restriction map of this genomic region was constructed. *pnut* cDNA clones were isolated from an eye–antennal imaginal disc library in λgt10 (made by A. Cowman) using genomic probes spanning the insertion site. The longest (2.5 kb) cDNA clone was subcloned into Bluescript KS II(+) (Stratagene) for further analysis.

RNA for blot analysis was prepared from a mixture of third instar imaginal discs as described (Moses et al., 1989), denatured and size fractionated (Berk and Sharp, 1977), blotted onto Magnagraph nylon membranes (Micron Separations), and probed with the digoxigenin-labeled cDNA subclone.

Plasmid DNA was sonicated and subcloned into M13mp10 for sequencing by the dideoxynucleotide chain termination method (Sanger et al., 1977) with the AutoRead kit (Pharmacia). Sequence reactions were analyzed on a Pharmacia LKB automated laser fluorescent DNA sequencer. The 2.5 kb *pnut* cDNA clone was sequenced on both strands. The precise sites of the P element insertion were determined by sequencing the junctions between P element and genomic DNA in the rescue plasmids, using a primer complementary to the 5′ end of the PZ element (5′-CCTCTCAACAAGCAAACGTGC-3′).

Data base searches and other sequence manipulations were performed with the Genetics Computer Group sequence analysis software package.

Transformation Rescue

A 10 kb BamHI fragment of genomic DNA containing the *pnut* transcription unit was cloned into the transformation vector pW8 (Klemenz et al., 1987). A second rescue construct consisted of a 1768 bp EcoRI–AflII fragment from the 2.5 kb *pnut* cDNA, cloned into the pCaSpeR-hs vector (Pirrotta, 1988). This vector contains the Drosophila *hsp70* promoter and 3′ untranslated region and provides heat-inducible expression. The resulting plasmids were injected into w^{1118} embryos as described (Karess and Rubin, 1984). Two transformant lines from each construct were established and crossed to $pnut^{XP}$ to assay rescue of the recessive lethality.

Antibody Production

Segments of the *pnut* gene were amplified by PCR and subcloned into the pGEX-3X (Smith and Johnson, 1988) and pRSET-C (Invitrogen) vectors to produce GST and His_6 fusion proteins. Three nonoverlapping segments were cloned: fusion I, amino acids 1–116; fusion II, amino acids 120–306; fusion III, amino acids 317–527. The resulting constructs were used to produce and purify bacterial fusion protein as described (Invitrogen protocol; Smith and Johnson, 1988). GST–pnut II and GST–pnut III fusion proteins were insoluble and were therefore run on SDS–polyacrylamide preparative gels and extracted from gel slices. Each GST fusion protein was injected into Swiss Webster mice, and antisera were tested for embryo staining and for ELISA reactivity to the His_6 fusion proteins (Harlow and Lane, 1988). Each serum produced a similar pattern of localization in embryos. Hybridoma cell line 4C9 was generated from a mouse immunized with GST–pnut fusion I. Specificity of MAb 4C9 was confirmed by two methods. First, protein immunoblots (Harlow and Lane, 1988) of third instar larvae extracts identified a single 4C9-positive band of 60 kDa that was present in extracts of wild-type larvae and absent in $pnut^-$ extracts. Second, mosaic tissues containing clones of $pnut^-$ cells generated by the FLP–FRT recombination system (Xu and Rubin, 1993) were stained with MAb 4C9. Eye–antennal discs of mosaic larvae contained patches of cells that did not stain with MAb 4C9, adjacent to twin spots of strongly staining cells.

Immunofluorescent Staining

Embryos were fixed and immunostained according to the protocol of Patel et al. (1987). S2 Drosophila culture cells were fixed on slides for 10 min in −70°C acetone and then processed for immunostaining as described (Patel et al., 1987) with wash and incubation times of 30 min. Ovaries were fixed and stained as described by Hay et al. (1990). Mouthhook–brain complexes with attached imaginal discs, lymph glands, and salivary glands were fixed and stained as described (Xu and Rubin, 1993). MAb 4C9 was used at a 1:4 dilution. Rabbit polyclonal serum 354, which is specific for Drosophila α-spectrin (Byers et al., 1987) was used at a 1:200 dilution. Rabbit anti-DMAP60 (a gift of D. Kellog) was used at 2 μg/ml. Texas red– and FITC-conjugated IgGs (Jackson Laboratories) were used at a 1:300 dilution. Nuclei were stained with Hoechst 33258 (0.5 μg/ml) or propidium iodide (10 μg/ml). To reduce background staining by propidium iodide, RNAase A (1 mg/ml) was included in some secondary antibody incubations. All tissues were mounted in Vectashield mounting medium (Vector Laboratories).

Microscopy

Confocal images were generated with a Zeiss confocal microscope and prepared for publication with Adobe Photoshop and Aldus Pagemaker software. Standard photomicrographs were prepared with a Zeiss Axiophot microscope.

Acknowledgments

We are indebted to Richard Carthew for advice and support during the early part of this work. We thank Linda Higgins for isolation of the *rN498* and *rQ348 pnut* alleles. We also thank Doug Kellog and Daniel Branton for antibodies and Johnny Fares and John Pringle for communicating results prior to publication and for performing the Lupas coiled-coil algorithm on the *pnut* sequence. Helpful comments on the manuscript were made by Zac Cande, David Drubin, and members of the Rubin laboratory. T. P. N. was supported by a National Science Foundation predoctoral fellowship.

Received February 9, 1994; revised March 10, 1994.

References

Berk, A. J., and Sharp, P. A. (1977). Sizing and mapping of early adenovirus mRNAs by gel electrophoresis of S1 endonuclease digested hybrids. Cell *12*, 721–732.

Byers, B., and Abramson, D. H. (1968). Cytokinesis in HeLa: post-telophase delay and microtubule-associated motility. Protoplasma *66*, 413–435.

Byers, B., and Goetsch, L. (1976a). A highly ordered ring of membrane-associated filaments in budding yeast. J. Cell Biol. *69*, 717–721.

Byers, B., and Goetsch, L. (1976b). Loss of the filamentous ring in cytokinesis-defective mutants of budding yeast. J. Cell Biol. *70*, 35a.

Byers, T. J., Dubreuil, R., Branton, D., Kiehart, D. P., and Goldstein, L. S. (1987). *Drosophila* spectrin. II. Conserved features of the α-subunit are revealed by analysis of cDNA clones and fusion proteins. J. Cell Biol. *105*, 2103–2110.

Carthew, R. W., and Rubin, G. M. (1990). *seven in absentia*, a gene required for specification of R7 cell fate in the Drosophila eye. Cell *63*, 561–577.

Chant, J., and Herskowitz, I. (1991). Genetic control of bud site selection in yeast by a set of gene products that constitute a morphogenetic pathway. Cell *65*, 1203–1212.

Edamatsu, M., Hirono, M., and Watanabe, Y. (1992). Tetrahymena profilin is localized in the division furrow. J. Biochem. *112*, 637–642.

Flescher, E. G., Madden, K, and Snyder, M. (1993). Components required for cytokinesis are important for bud site selection in yeast. J. Cell Biol. *122*, 373–386.

Ford, S. K., and Pringle, J. R. (1991). Cellular morphogenesis in the *Saccharomyces cerevisiae* cell cycle: localization of the *CDC11* gene product and the timing of events at the budding site. Dev. Genet. *12*, 281–292.

Franceschini, N., and Kirschfeld, K. (1971). Les phénomenes de pseudopille dans l'oeil composé de *Drosophila*. Kybernetiks *9*, 159–182.

Gatti, M., and Baker, B. S. (1989). Genes controlling essential cell-cycle functions in *Drosophila melanogaster*. Genes Dev. *3*, 438–453.

Haarer, B. K., and Pringle, J. R. (1987). Immunofluorescence localization of the *Saccharomyces cerevisiae CDC12* gene product to the vicinity of the 10-nm filaments in the mother-bud neck. Mol. Cell. Biol. *7*, 3678–3687.

Harlow, E., and Lane, D. (1988). Antibodies: A Laboratory Manual (Cold Spring Harbor, New York: Cold Spring Harbor Laboratory Press).

Hartwell, L. H. (1971). Genetic control of the cell division cycle in yeast. IV. Genes controlling bud emergence and cytokinesis. Exp. Cell. Res. *69*, 265–271.

Hartwell, L. H. (1974). *Saccharomyces cerevisiae* cell cycle. Bacteriol. Rev. *38*, 164–198.

Hay, B., Jan, L. Y., and Jan, Y. N. (1990). Localization of *vasa*, a component of *Drosophila* polar granules, in maternal-effect mutants that alter embryonic anteroposterior polarity. Development *109*, 425–433.

Hime, G., and Saint, R. (1992). Zygotic expression of the *pebble* locus is required for cytokinesis during the postblastoderm mitoses of *Drosophila*. Development *114*, 165–171.

Hooper, J. E., and Scott, M. P. (1989). The Drosophila *patched* gene encodes a putative membrane protein required for segmental patterning. Cell *59*, 751–765.

Karess, R. E., and Rubin, G. M. (1984). Analysis of P transposable element functions in Drosophila. Cell *38*, 135–146.

Karess, R. E., Chang, X., Edwards, K. A., Kulkarni, S., Aguilera, I., and Kiehart, D. P. (1991). The regulatory light chain of nonmuscle myosin is encoded by *spaghetti-squash*, a gene required for cytokinesis in Drosophila. Cell *65*, 1177–1189.

Kato, K. (1991). Sequence analysis of twenty mouse brain cDNA clones selected by specific expression patterns. J. Neurosci. *2*, 704–711.

Kim, H. B., Haarer, B. K., and Pringle, J. R. (1991). Cellular morphogenesis in the *Saccharomyces cerevisiae* cell cycle: localization of the *CDC3* gene product and the timing of events at the budding site. J. Cell Biol. *112*, 535–544.

Klemenz, R., Weber, U., and Gehring, W. J. (1987). The *white* gene as a marker in a new P-element vector for gene transfer in *Drosophila*. Nucl. Acids Res. *15*, 3947–3959.

Lehner, C. F. (1992). The *pebble* gene is required for cytokinesis in *Drosophila*. J. Cell Sci. *103*, 1021–1030.

Lupas, A., Van Dyke, M., and Stock, J. (1991). Predicting coiled coils from proteins sequences. Science *252*, 1162–1164.

Mlodzik, M., and Hiromi, Y. (1991). The enhancer trap method in *Drosophila*: its application to neurobiology. Meth. Neurosci. *9*, 397–414.

Moses, K., Ellis, M. C, and Rubin, G. M. (1989). The *glass* gene encodes a zinc-finger protein required by *Drosophila* photoreceptor cells. Nature *340*, 531–536.

Mullins, J. M., and Biesele, J. J. (1977). Terminal phase of cytokinesis in D-98S cells. J. Cell Biol. *73*, 672–684.

Mullins, M. C., and Rubin, G. M. (1991). Isolation of temperature-sensitive mutations of the tyrosine kinase receptor *sevenless* (*sev*) in *Drosophila* and their use in determining its time of action. Proc. Natl. Acad. Sci. USA *88*, 9387–9391.

Nottenburg, C., Gallatin, W. M., and St. John, T. (1990). Lymphocyte HEV adhesion variants differ in the expression of multiple gene sequences. Gene *95*, 279–284.

O'Kane, C. J., and Gehring, W. J. (1987). Detection *in situ* of genomic regulatory elements in *Drosophila*. Proc. Natl. Acad. Sci. USA *84*, 9123–9127.

Patel, N., Snow, P. M., and Goodman, C. S. (1987). Characterization and cloning of fasciclin III: a glycoprotein expressed on a subset of neurons and axon pathways in Drosophila. Cell *48*, 975–988.

Pickett-Heaps, J. D., and Northcote, D. H. (1966). Organisation of microtubules and endoplasmic reticulum during mitosis and cytokinesis in wheat meristems. J. Cell Sci. *1*, 109–120.

Pirrotta, V. (1986). Cloning *Drosophila* genes. In *Drosophila*: A Practial Approach, D. R. Roberts, ed. (Washington, D. C.: IRL Press), pp. 83–110.

Pirrotta, V. (1988). Vectors for P-mediated transformation in *Drosophila*. In Vectors: A Survey of Molecular Cloning Vectors and Their Uses, R. L. Rodriguez and D. T. Denhardt, eds. (Boston: Butterworth), pp. 437–456.

Rappaport, R. (1986). Establishment of the mechanism of cytokinesis in animal cells. Int. Rev. Cytol. *105*, 245–281.

Rickoll, W. L., and Counce, S. J. (1980). Morphogenesis in the embryo of *Drosophila melanogaster*: germ band extension. Roux's Arch. Dev. Biol. *188*, 163–177.

Robertson, H. M., Preston, C. R., Phillis, R. W., Johnson-Schlitz, D. M., Benz, W. K., and Engels, W. R. (1988). A stable genomic source of P element transposase in *Drosophila melanogaster*. Genetics *118*, 461–470.

Sanger, F., Nicklen, S., and Coulson, A. (1977). DNA sequencing with chain-terminating inhibitors. Proc. Natl. Acad. Sci. USA *86*, 8333–8337.

Sanger, J. M., Pochapin, M. B., and Sanger, J. W. (1985). Midbody sealing after cytokinesis in embryos of the sea urchin *Arabacia punctulata*. Cell Tissue Res. *240*, 287–292.

Saraste, M., Sibbald, P. R., and Wittinghofer, A. (1990). The P-loop: a common motif in ATP- and GTP-binding proteins. Trends Biochem. Sci. *15*, 430–434.

Schejter, E. D., and Wieschaus, E. (1993). Functional elements of the cytoskeleton in the early *Drosophila* embryo. Annu. Rev. Cell Biol. *9*, 67–99.

Schroeder, T. E. (1972). The contractile ring. II. Determining its brief existence, volumetric changes and vital role in cleaving *Arbacia* eggs. J. Cell Biol. *53*, 419–434.

Schroeder, T. E. (1990). The contractile ring and furrowing in dividing cells. Ann. NY Acad. Sci. *582*, 78–87.

Smith, D. B., and Johnson, K. S. (1988). Single-step purification of polypeptides expressed in *Escherichia coli* as fusions with glutathione S-transferase. Gene *67*, 31–40.

Snyder, M., Gehrung, S., and Page, B. D. (1991). Studies concerning the temporal and genetic control of cell polarity in *Saccharomyces cerevisiae*. J. Cell Biol. *114*, 515–532.

Wolff, T., and Ready, D. (1991). The beginning of pattern formation in the *Drosophila* compound eye: the morphogenetic furrow and the second mitotic wave. Development *113*, 841–850.

Xu, T., and Rubin, G. M. (1993). Analysis of genetic mosaics in developing and adult *Drosophila* tissues. Development *117*, 1223–1237.

Yonemura, S., Mabuchi, I., and Tsukita, S. (1991). Mass isolation of cleavage furrows from dividing sea urchin eggs. J. Cell Sci. *100*, 73–84.

Zipursky, S. L., and Rubin, G. M. (1994). Determination of neuronal cell fate: lessons from the R7 neuron of *Drosophila*. Annu. Rev. Neurosci. *17*, 373–397.

GenBank Accession Number

The accession number for the sequence reported in this paper is U08103.